Inorg. Chem. **2002**, *41*, 5961–5967

Nonstoichiometric Spinel Ferrites Obtained from α-$NaFeO_2$ via Molten Media Reactions

Emilio Morán,*,† Mª Carmen Blesa,† M.-Eloisa Medina,† Jesús D. Tornero,‡ Nieves Menéndez,‡ and Ulises Amador§

Dpto. Química Inorgánica, Fac. CC. Químicas, Universidad Complutense, 28040-Madrid, Spain, Dpto. Química-Física Aplicada, Fac. Ciencias Universidad Autónoma, Cantoblanco, 28049-Madrid, Spain, and Fac. CC. Experimentales y Técnicas, Universidad San Pablo CEU, 28668- Madrid, Spain

Received December 20, 2001

Different solid/liquid "exchange" reactions involving divalent cations, protons, or ammonium ions have been performed at low/moderate temperatures (between 80 and 500 °C) on α-$NaFeO_2$ dipped in molten salts (or acid) media. Several ferrites have been obtained which are nonstoichiometric with partially inverse spinel structures. When sodium is replaced by divalent cations (Mg^{2+}, Co^{2+}, Ni^{2+}, and Zn^{2+}), the obtained ferrites are hyperstoichiometric (cation/oxygen ratio higher than 3/4) whereas proton or ammonium reactions result in hypostoichiometric materials (cation/oxygen lower than 3/4). All these ferrites present a platelet-like morphology and show ferrimagnetic, soft magnet behavior.

1. Introduction

Ferrites are ceramic oxides where Fe_2O_3 is a major component and are widely studied because of their outstanding magnetic properties. Although different structures may be displayed, the spinel one is quite common among ferrites. Most spinel-ferrites present the ideal stoichiometry, MFe_2O_4, where M accounts for a divalent metal and the cation/anion ratio is 3/4, but one of the most interesting spinel-ferrites, γ-Fe_2O_3, maghemite, is far from this stoichiometry, because of the presence of cationic vacancies. These materials are soft magnets with low coercitivies and high resistivities, both properties leading to industrial applications in microwave devices, satellite communications, transformers, audio−video and digital recording, and so forth.[1−3]

Usually, ferrite materials are synthesized by one of two major routes: either by a traditional ceramic method or by coprecipitation[4] or a sol−gel-type[5,6] process. As is usual in materials chemistry, the magnetic and electrical properties are sensitive to the synthesis and processing conditions, and moderate or low temperature synthetic procedures, such as the thermolysis of precursors, are gaining interest.[7] An alternative, relatively little explored, route to prepare ferrites is based on cationic exchange reactions performed at moderate temperatures.

A suitable inorganic solid for cationic exchange reactions should contain mobile ions and have an open structure (interconnected cages, channels, or layers of sufficient dimensions to allow ion transport). In addition, an effective liquid reaction medium is also needed, and aqueous solutions, organic acids, or molten inorganic salts (either pure or eutectic mixtures) can be used. Taking into account the moderate temperatures at which these reactions are usually performed, and realizing that extensive parts of the framework are retained, these processes can be considered as a "chimie douce" method of preparation for which structural, thermodynamic, and kinetic constraints are very important.[8,9] The sodium ferrite, α-$NaFeO_2$ with a rhombohedral rock-salt superstructure, space group $R\bar{3}m$ (Figure 1A), satisfies

* To whom correspondence should be adressed. E-mail: emoran@quim.ucm.es. Phone: 34-913944234. Fax: 34-913944352.
† Fac. CC. Químicas, Universidad Complutense.
‡ Fac. Ciencias Universidad Autónoma.
§ Fac. CC. Experimentales y Técnicas, Universidad San Pablo CEU.

(1) Snelling, E. C. *Soft Ferrites*, 2nd ed.; Butterworth: London, 1988.
(2) Smith, J.; Wijn, H. P. J. *Ferrites*; Wiley: New York, 1959.
(3) Sugimoto, M. *J. Am. Ceram. Soc.* **1999**, *82*, 269.
(4) Goldman, A.; Lairy, A. M. *J. Phys.* **1976**, *4*, C1.
(5) Livage, J.; Henry, M.; Sánchez, C. *Prog. Solid State Chem.* **1998**, *18*, 259.
(6) Chatterjee, D.; Pas, S.; Pradhan, K.; Chakravorty, D. *J. Magn. Mater.* **1993**, *127*, 214.
(7) Randhawa, S. *J. Mater. Chem.* **2000**, *10*, 2847.
(8) England, W. A.; Goodenough, J. B.; Wiseman, X. *J. Solid State Chem.* **1983**, *49*, 289.
(9) Durand, B.; Paris, J. M.; Escoubes, M. *Ann. Chim. (Paris)* **1978**, *3*, 135.

10.1021/ic011302k CCC: $22.00
Published on Web 10/18/2002

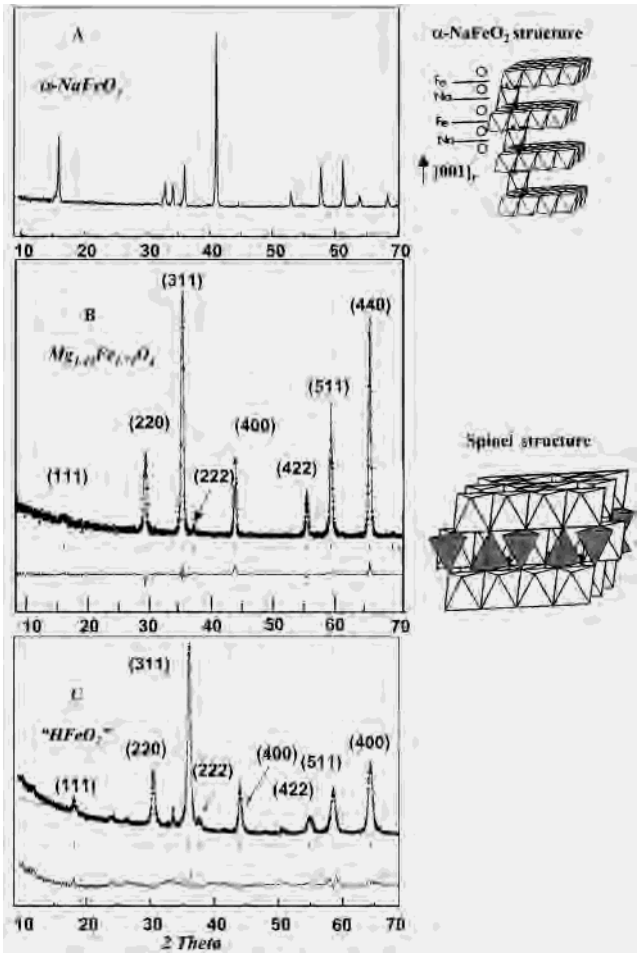

Figure 1. XRD patterns of α-$NaFeO_2$ (A), magnesium ferrite (B), and $HFeO_2$ (C). Polyhedral representations of the α-$NaFeO_2$ and spinel structures are depicted. The α-$NaFeO_2$ [001] direction is equivalent to the [111] spinel one.

the conditions for these kind of reactions: the structure may be considered as bidimensional, and the sodium mobility in this compound is appreciable (5×10^{-5} S·cm^{-1} at 500 K) as shown by ionic conductivity measurements.[10] It should also be noted that the bonding in the iron-oxide layers is largely covalent, because of the high charge/radius ratio of Fe^{3+}, in contrast to the sodium-oxide layers which are more ionic, implying that Na^+/M^{x+}, "exchange" reactions, should preserve the [FeO_6] octahedral layers.

In this paper, we propose a "cationic exchange" method, performed on α-$NaFeO_2$ at low temperatures, as a general, "chimie douce" route, to obtain ferrites. Previously obtained results are reviewed[11−13] and compared with new ones. By these means, we have obtained nonstoichiometric spinels, either hyper- or hypostoichiometric, depending on the cation/anion ratio achieved (higher or lower than 3/4, respectively). All these materials show a partially inverse spinel structure and are ferrimagnetic. Finally, and taking into account that the α-$NaFeO_2$ structure is a quite common one, the procedure could be extended to similar oxides (i.e., $LiCoO_2$, widely used in rechargeable lithium batteries, which shows this structure[14]) and could provide an avenue to new nonferritic materials.

2. Experimental Section

2.1. Synthesis. The precursor α-$NaFeO_2$ was prepared according to the method outlined by Takeda et al.[15] and involved repeated heat treatments (24 h, 400−500 °C) of pelleted mixtures of sodium peroxide and hematite. In contrast with ceramic methods that yield mixtures of phases (α-$NaFeO_2$ and β-$NaFeO_2$), basically this method produces only the α polymorph. This oxide was subsequently used in three types of reactions outlined here:. (a) For the reactions with divalent cations M^{2+} (M = Mg, Co, Ni, Zn), molten eutectic mixtures of the corresponding chlorides and KCl were used as reaction media. In each case, the eutectic mixture with lowest melting point was chosen.[16] In a typical experiment, a weight ratio of 1/5 (α-$NaFeO_2$/eutectic) was used with a reaction time of 48 h at 500 °C. An alternative way was using molten nitrates such as $NaNO_3$ (mp 334 °C) as the molten media with the stoichiometric amount of a divalent nitrate added as reactant. Although the reactions can be performed in open vessels, best results were obtained when performed in sealed Pyrex ampules. The obtained products were washed with distilled water until no chlorides (or nitrates, if this was the choice for molten salts) were detected by chemical analysis, then filtered, and air-dried in an oven. (b) The sodium/proton "exchange" reactions were performed employing molten benzoic acid, HBz (mp = 122 °C), at 150 °C for 24 h either in an open (room pressure) flask, or in a sealed Pyrex ampule, the best materials being obtained in the second case. A typical reaction used 1 g of α-$NaFeO_2$ and 50 g of benzoic acid, the mixture being stirred and most of the remaining acid being decanted upon finishing the experiment. The solid product was throughly washed by a flow-back treatment with methanol in a first step and with hot water in a second one. (c) For the sodium/ammonium reactions, NH_4NO_3 was used in the molten state at 200 °C, in open containers, only in small amounts, less than 10 g, to avoid explosion hazards (WARNING!). Again, 48 h was the usual reaction time, after which the products were thoroughly washed and filtered.

2.2. Characterization. Powder X-ray diffraction patterns were recorded using a Siemens D-5000 apparatus (Bragg−Brentano geometry), employing a monochromatic beam, Cu Kα radiation (λ = 1.5418 Å filtered with Ni), and operating in the step scan technique, with a step size of 0.02° and a step time of 15 s/step; 2θ range was between 10° and 70°. One of the nickel ferrites was also previously characterized by means of neutron diffraction, and the corresponding results were published elsewhere.[12] Data were refined, in most cases, by means of the FULLPROF program[17] based on the Rietveld method. Profiles were fitted by using a pseudo-Voight function. The occupancies of the different crystallographic sites are not independent as some restrictions were

(10) Blesa, M. C.; Morán, E.; León, C.; Santamaría, J.; Tornero, J. D.; Menéndez, N. *Solid State Ionics* **1999**, *126*, 81.
(11) Blesa, M. C.; Amador, U.; Morán, E.; Menéndez, N.; Tornero, J. D.; Rodríguez-Carvajal, J. *Solid State Ionics* **1993**, *63*−*65*, 429.
(12) Blesa, M. C.; Morán, E.; Amador, U.; Andersen, N. H. *J. Solid State Chem.* **1997**, *129*, 123.
(13) Blesa, M. C.; Morán, E.; Tornero, J. D.; Menéndez, N.; Mata-Zamora, E.; Saníger, J. M. *J. Mater. Chem.* **1999**, *9*, 227.
(14) *Handbook of Batteries Materials*; Besenhard, J. O., Ed.; Wiley-VCH: New York, 1999; Chapter III, p 300.
(15) Takeda, Y.; Agaki, J.; Edagawa, A.; Ainagaki, M.; Naka, S. *Mater. Res. Bull.* **1980**, *15*, 1167.
(16) *Phase Equilibria Diagrams Database*; American Ceramic Society: 1998.
(17) Rodríguez-Carvajal, J. FULLPROF: A Program for Rietveld Refinement and Pattern Matching Analysis. *Abstracts of the Satellite Meeting of the 15th Congress of the International Union of Crystallography*; Toulouse, France, 1990; 127.

Table 1. Chemical Compositions as Deduced from ICP Analysis for Hyperstoichiometric $M_{1+x}Fe_{2-2/3x}O_4$ Spinels

M	Fe/M[a]	*x*	composition
Mg	1.20	0.43	$Mg_{1.43}Fe_{1.71}O_4$
Co	1.69	0.13	$Co_{1.13}Fe_{1.91}O_4$
Ni	1.48	0.35	$Ni_{1.25}Fe_{1.85}O_4$
Zn	1.75	0.10	$Zn_{1.10}Fe_{1.93}O_4$

[a] Experimental atomic ratio. Na^+ content is in all cases less than 1%.

imposed to meet the chemical and Mössbauer analysis results; oxygen stoichiometry has been always fixed as 4.0 based on our previous results obtained by means of neutron diffraction for a nickel ferrite.[12] In this XRD work, thermal factors were refined overall, because the low scattering factor for oxygen does not allow more precise work.

Chemical analysis was performed by inductive coupled plasma (ICP). Magnetization measurements were made at room temperature. Mössbauer spectra were collected on a conventional spectrometer working at a constant acceleration mode with ^{57}Co in a rhodium matrix as radioactive source. The particle morphology of the samples was studied by scanning electron microscopy (SEM). IR spectra were recorded in a Nicolet 5SX apparatus fitted with cesium iodide optics, samples being diluted in KBr for transmission experiments.

3. Results and Discussion

As shown by powder XRD analysis, all the products had the spinel structure. Some representative samples were analyzed by ICP to know the final composition: in all cases, only small amounts (<1%) of remnant sodium were detected, meaning that the degree of reaction achieved was close to 100%. Therefore, the actual chemical compositions of the samples obtained have to be compared with the ideal MFe_2O_4, and according to this, they fall into two categories: hyper- or hypostoichiometric ferrites.

3.1. Hyperstoichiometric Materials. ICP chemical analysis, Table 1, confirms the quantitative nature of the "exchange" reactions, ideally formulated as

$$2\alpha\text{-}NaFeO_2(s) + MX_2(l) \rightarrow MFe_2O_4(s) + 2NaX(l) \quad (1)$$

$$(M^{II} = Mg, Co, Ni, Zn; X = Cl^- \text{ or } NO_3^-)$$

with the reaction being driven by the very favorable formation enthalpy of the sodium salt ($2\Delta H°_f(NaX)$ as compared to $\Delta H°_f(MX_2)$), if the formation enthalpies per iron of the ferrites are supposed to be similar. The reaction via chlorides yields more pure ferrites because the nitrates route also produces some hydrolysis products (the divalent nitrates are always hydrated). Nevertheless, if molten chlorides are used as reaction media, at 500 °C, a small amount of iron, not only sodium, is also extracted from the material; therefore, a bigger than expected amount of the divalent cation enters the structure, and the global reaction can be schematized as

$$2\alpha\text{-}NaFeO_2(s) + (1+x)MCl_2(l) \rightarrow M_{1+x}Fe_{2-2/3x}O_4(s) + 2NaCl(l) + 2x/3FeCl_3(l) \quad (2)$$

$$(M^{II} = Mg, Co, Ni, Zn)$$

Table 2. Structural Relationships between Atacamite, Spinel, Halite, and α-$NaFeO_2$

structure type	simplified formula	cell param	occupied positions[a] octahedral	occupied positions[a] tetrahedral
atacamite $Cu_2(OH)_3Cl$	B_2O_4	2*a*	16d	
spinel	AB_2O_4	2*a*	16d	8a
halite	$(A,B)O \equiv (A,B)_4O_4$	*a*	16d + 16c	
α-$NaFeO_2$	$ABO_2 \equiv A_2B_2O_4$	$a/\sqrt{2}$	16d + 16c	

[a] These positions refer to the *Fd*3*m* space group.

From the structural point of view, the reaction is not a true ion-exchange process because the original α-$NaFeO_2$ structure is not preserved but transforms to a spinel structure, Figure 1B, and this is the reason to use the word "exchange" with quotation marks. Nevertheless, at the working temperatures used, this is not a dissolving−recrystallizing process: the solid always remains separated as a different phase. The transformation is possible because there are close structural relationships between the framework of both structures, something that can be intuitively inferred from the polyhedral schemes of Figure 1. All the available octahedral positions are occupied in α-$NaFeO_2$, and all the tetrahedral ones are empty, while $^1/_8$ of the tetrahedral sites and $^1/_2$ of the octahedral ones are occupied in the spinel. In fact, both structures have in common an octahedral "atacamite" B_2O_4 framework[12,18] based on a cubic close packing of O^{2-}. If we refer the three structures (atacamite, spinel, and halite) to a unit cell containing 32 oxygen anions, this will produce 32 octahedral holes (16c and 16d using the Wyckoff notation of the *Fd*3*m* space group) and 64 tetrahedral holes (8a, 8b, and 48f). These structural relationships are summarized in Table 2.

Therefore, the "exchange" reactions involve important structural rearrangements: some Fe^{3+} cations should leave their initial octahedral positions and move to the empty adjacent tetrahedral ones, and the entering M^{2+} cations should go to the octahedral sites initially occupied by sodium. As a result of this mechanism, all the spinels obtained have a partially inverse character.

Mössbauer analysis was used to confirm the iron oxidation state (Fe^{3+}) and its distribution in octahedral and tetrahedral positions. Figure 2A shows a room temperature spectrum of a representative material ($Mg_{1.43}Fe_{1.71}O_4$) with two magnetic hyperfine-field values for the tetra- and octahedral sites. If we suppose a random distribution for Mg and Fe ions in both tetra- and octahedral positions, we can deduce the occupation of the different crystallographic sites from the Mössbauer spectra and the X-ray diffraction data. The distribution of iron between the octahedral and tetrahedral sites can be established; in this sample, about 60% of iron ions are located in tetrahedral sites, while the rest occupy the octahedral positions. Taking into account these results, divalent cations (Mg^{2+}) should be mainly located in octahedral sites. This is in reasonably good agreement with the complex cationic distribution observed in this material by X-ray diffraction (55% of iron in tetrahedral sites) and can

(18) Wells, A. F. *Structural Inorganic Chemistry*, 4th ed.; Clarendon Press: Oxford, 1975; p 490.

Table 3. Cell Parameters, Iron Distributions, and Magnetic Moments of Some Hyperstoichometric Spinels

		population Fe^{3+} [a]		population Fe^{3+} [b]		magnetic moment[c]	
composition	cell param (Å)	octahedral	tetrahedral	octahedral	tetrahedral	$\mu_{exp}(\mu_B)$	$\mu_{calcd}(\mu_B)$
$Mg_{1.43}Fe_{1.71}O_4$	8.392(2)	40.0%	60.0%	45.0%	55.0%	0.94	0.94
$Co_{1.13}Fe_{1.91}O_4$	8.403(2)	43.0%	57.0%	53.40%	46.6%	3.25	3.32
$Ni_{1.25}Fe_{1.85}O_4$	8.342(3)	44.0%	56.0%	50.3%	49.7%	1.85	2.09
$Zn_{1.10}Fe_{1.93}O_4$	8.443(3)	44.6%	55.4%	49.0%	51.0%	0.22	0.20

[a] Data obtained by Mössbauer spectroscopy. [b] According to XRD data. [c] Magnetic moments calculated by using the Néel collinear model.

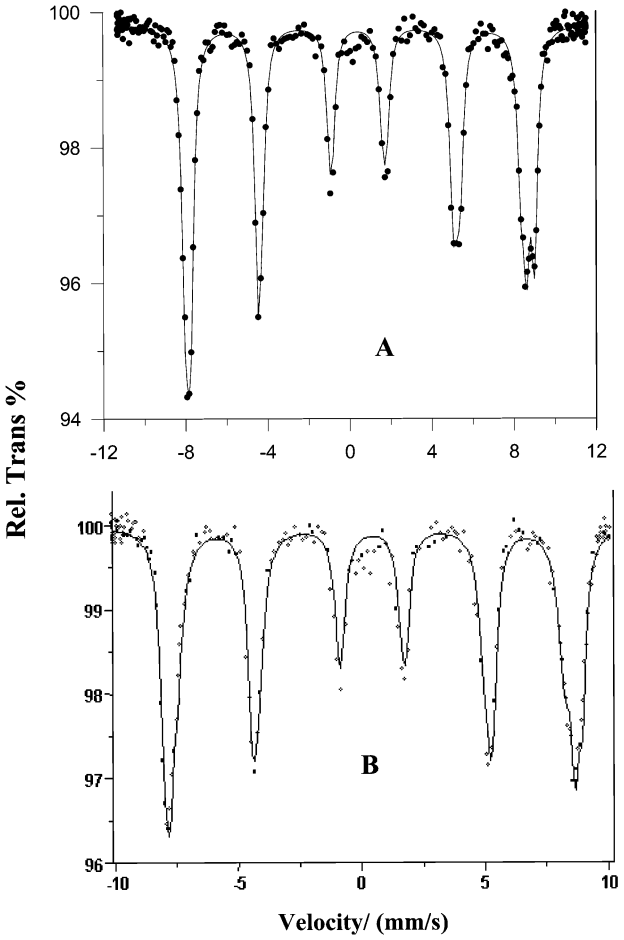

Figure 2. Room temperature Mössbauer spectra of $Mg_{1.43}Fe_{1.71}O_4$ (A) and $Fe_zO_{3z-4}(OH)_{8-3z}$ (B); $z = 12/5$.

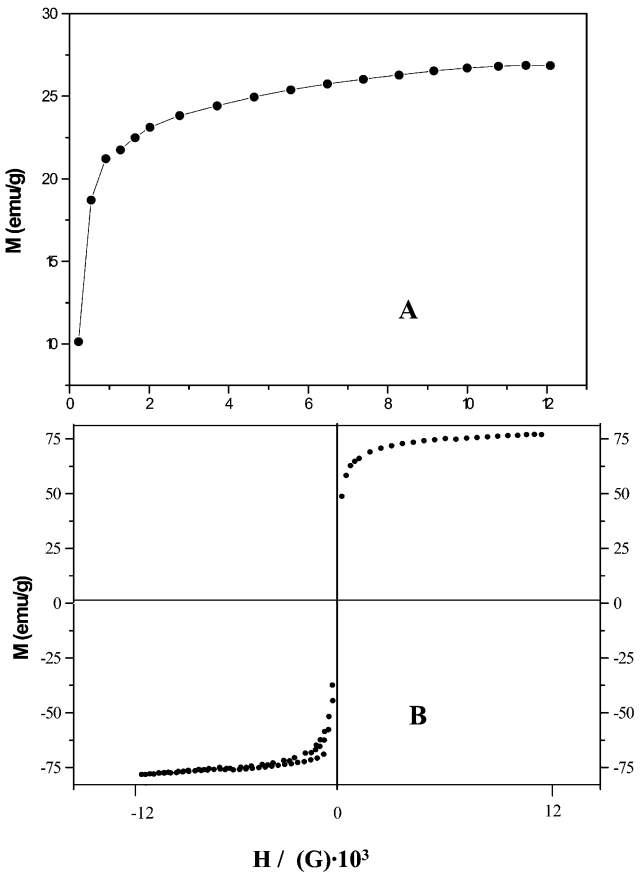

Figure 3. Magnetic measurements of $Mg_{1.43}Fe_{1.71}O_4$ (A) and $Fe_zO_{3z-4}(OH)_{8-3z}$ (B); $z = 12/5$.

also be extended to the nickel and zinc ferrites. Nevertheless, in the case of the cobalt ferrite, some discrepancies between the Mössbauer and the X-ray deduced populations are observed; magnetic measurements seem to better fit the XRD data.

In the magnetization versus temperature curve of the magnesium sample, which is presented in Figure 3A, the ferrimagnetic character of this material can be seen. The experimental effective magnetic moments per formula unit of all ferrites studied are in good agreement with the calculated ones, assuming the Néel collinear model ($\mu_{calcd} = [A]_{tet}[B]_{oct}$), where A and B account for the different magnetic cations occupying those sites; the iron distribution was used as deduced from Mössbauer analysis. Cell parameters, magnetic moments, and iron distributions are indicated in Table 3. Zn^{2+} "exchange" is particularly interesting because ceramic procedures produce zinc ferrite with the normal spinel distribution which is therefore antiferromagnetic. In contrast, the "exchange" route results in a partially inverse structure and ferrimagnetic properties as indicated by the magnetization versus applied field behavior (Figure 4A). The Curie transition temperature of this material can be graphically estimated from an inverse susceptibility versus temperature plot, as shown in Figure 4B. This unusual behavior has also been studied for a zinc ferrite obtained by Warren B. Cross et al.[19] by a quite different, "soft" procedure.

It is interesting to note that the Rietveld analysis of neutron diffraction data of a nickel ferrite, published elsewhere,[12] revealed that the octahedral sites 16c, which are empty in the ideal stoichiometric spinels, are partially occupied. In that case, to achieve the maximum resolution for the refinement of the nuclear structure, neutrons of a short wavelength, 1.066(1) Å, were chosen, and the oxygen stoichiometry was independently refined until convergence was reached for a

(19) Cross, W. B.; Affleek, L. M.; Kuznetsov, Y.; Parkin, I. P.; Pankhurst, Q. A. *J. Mater. Chem.* **1999**, *9*, 2545−2552.

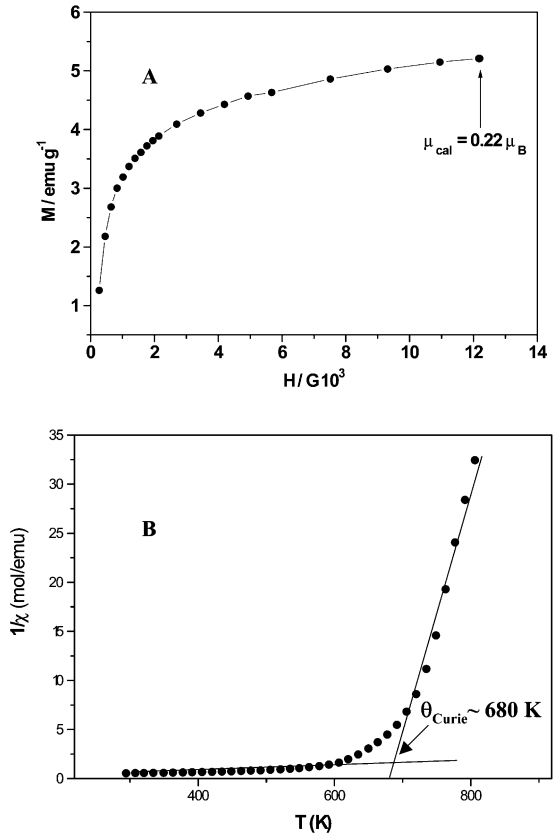

Figure 4. Magnetization, *M*, vs applied magnetic field, *H*, (A) and inverse susceptibility vs temperature, *T*, (B) plots for $Zn_{1.10}Fe_{1.92}O_4$.

total occupancy of the anionic sublattice. On the grounds of that neutron diffraction analysis, the results presented here have been obtained by applying the same model, although with XRD data, assuming the occupation by divalent cations, in a disordered way, of some of the usually empty octahedral 16c sites within a complete oxide framework (more work using neutron diffraction for the remaining samples is in progress). Table 4 collects XRD data corresponding to several hyperstoichometric spinels (magnesium, cobalt, nickel, and zinc ferrites). Concerning this feature, it could be argued that the occupation by two cations of adjacent tetrahedra and octahedra, which share one face, would result in strong electrostatic repulsions (i.e., the distance between Mg^{2+} in a 16c site and Fe^{3+} in an 8a site is 1.81 Å), but this being true, this possibility has already been theoretically considered by Kesler and Filimonov[20] who concluded that a few intermediate structures in the atacamite−spinel−halite series would be stable enough to be formed. In our opinion, our ferrites fall in one of the possible cases. Moreover, this kind of interstitial occupation of some of the 16c sites, being disordered and in small concentration, would produce, because of the cation−cation repulsions, only local distortions of the structure around these point defects, and neither neutron nor X-ray diffraction, being macroscopic, average techniques, would detect these microstructural features.

3.2. Hypostoichiometric Materials. If molten benzoic acid is used as reaction medium, replacement of Na^+ by protons occurs, and this can be considered as an acid−base type of reaction.[13,21] This process has been exemplified by K. R. Poeppelmeier et al., working on aluminates.

Again, ICP analysis confirmed that the "exchange" was essentially complete because only small amounts of sodium remained in the reaction products. Similar types of reactions cannot be performed in aqueous media because α-$NaFeO_2$ is then readily hydrolyzed.[22] The process can be expressed as

$$\alpha\text{-}NaFeO_2 + HBz \rightarrow \text{“}HFeO_2\text{”} + NaBz$$

If molten ammonium nitrate is used, ammonia vapors are produced, and the expected ammonium ferrite cannot be isolated (either it is never produced or it instantly decomposes). The proposed process in this case could be decomposed in two steps (never observed independently) as follows:

$$\alpha\text{-}NaFeO_{2(s)} + NH_4NO_3 \rightarrow \text{“}NH_4FeO_2\text{”} + NaNO_3 \quad (1)$$

$$\text{“}NH_4FeO_2\text{”} \rightarrow 1/z\square_{3-z}Fe_zO_{3z-4}(OH)_{8-3z} + NH_3 + (2-4/z)H_2O \qquad (2 \le z \le {}^8/_3) \quad (2)$$

The "exchange" reaction proposed in step 1 may be considered unlikely on size grounds: the radius of NH_4^+

Table 4. Rietveld Analysis of Some Hyperstoichometric Spinels

atom	site	*x*/*a*	*y*/*b*	*z*/*c*	occupancy
		Magnesium Ferrite ($Mg_{1.43}Fe_{1.71}O_4$)[a]			
Mg	8a	0.0	0.0	0.0	0.06(1)
Fe	8a	0.0	0.0	0.0	0.94(1)
Fe	16d	5/8	5/8	5/8	0.77(2)
Mg	16d	5/8	5/8	5/8	1.23(2)
Mg	16c	1/8	1/8	1/8	0.14(2)
O	32e	*u*	*u*	*u*	4.00
		Cobalt Ferrite ($Co_{1.13}Fe_{1.91}O_4$)[b]			
Fe	8a	0.0	0.0	0.0	0.88(1)
Co	16d	5/8	5/8	5/8	0.94(1)
Fe	16d	5/8	5/8	5/8	1.02(1)
Co	16c	1/8	1/8	1/8	0.19(1)
O	32e	*u*	*u*	*u*	4.00
		Nickel Ferrite ($Ni_{1.25}Fe_{1.85}O_4$)[c]			
Fe	8a	0.0	0.0	0.0	0.92(1)
Ni	16d	5/8	5/8	5/8	1.07(1)
Fe	16d	5/8	5/8	5/8	0.93(1)
Ni	16c	1/8	1/8	1/8	0.18(1)
O	32e	*u*	*u*	*u*	4.00
		Zinc Ferrite ($Zn_{1.10}Fe_{1.93}O_4$)[d]			
Zn	8a	0.0	0.0	0.0	0.06(1)
Fe	8a	0.0	0.0	0.0	0.94(1)
Zn	16d	5/8	5/8	5/8	1.02(1)
Fe	16d	5/8	5/8	5/8	0.98(1)
O	32e	*u*	*u*	*u*	4.00

[a] Cell parameters: $a_0 = 8.392(2)$ Å; $u = 0.382(2)$. Agreement factors: $R_P = 14\%$; $R_{wp} = 19.4\%$; $R_{exp} = 11.5\%$; $R_B = 5.36\%$; $\chi^2 = 2.88$; B_{over} (Å²) = 1.25(6). [b] Cell parameters: $a_0 = 8.403(2)$ Å; $u = 0.381(1)$. Agreement factors: $R_P = 15.6\%$; $R_{wp} = 19.9\%$; $R_{exp} = 8.82\%$; $R_B = 7.71\%$; $\chi^2 = 5.10$; B_{over} (Å²) = 0.68(2). [c] Cell parameters: $a_0 = 8.342(3)$ Å; $u = 0.380(2)$. Agreement factors: $R_P = 13.6\%$; $R_{wp} = 17.5\%$; $R_{exp} = 8.72\%$; $R_B = 7.65\%$; $\chi^2 = 2.88$; B_{over} (Å²) = 0.40(2). [d] Cell parameters: $a_0 = 8.443(3)$ Å; $u = 0.382(2)$. Agreement factors: $R_P = 13.8\%$; $R_{wp} = 17.7\%$; $R_{exp} = 8.69\%$; $R_B = 8.17\%$; $\chi^2 = 4.13$; B_{over} (Å²) = 1.28(2).

(20) Kesler, Y. A.; Filimonov, D. S. *Inorg. Mater.* **1994**, *30*, 1255.

(21) Poeppelmeier, K. R.; Kipp, D. O. *Inorg. Chem.* **1988**, *27* (5), 766.

(22) Blesa, M. C.; Morán, E.; Menéndez, N.; Tornero, J. D.; Torrón, C. *Mater. Res. Bull.* **1993**, *28*, 837.

Table 5. Cell Parameters, Iron Distributions, and Magnetic Moments of Some Hypostoichometric Materials

		population Fe^{3+} [a]		population Fe^{3+} [b]		magnetic moment[c]	
composition	cell param (Å)	octahedral	tetrahedral	octahedral	tetrahedral	μ_{exp} (μ_B)	μ_{calcd} (μ_B)
$HFeO_2$ [13]	8.362(2)	56%	44%	57%	43%	0.74	0.70
$Fe_zO_{3z-4}(OH)_{8-3z}$, $z = 12/5$	8.332(2)	58%	42%			4.56	4.00

[a] Data obtained by Mössbauer spectroscopy. [b] According to XRD data. [c] Magnetic moment calculated using the Néel collinear model.

Table 6. Rietveld Analysis of a Hypostoichiometric Material Obtained by "Exchange" Reaction in Molten Benzoic Acid

composition	atom	site	*x*/*a*	*y*/*b*	*z*/*c*	occupancy
$HFeO_2$[a]	Fe	8a	0.0	0.0	0.0	0.86(1)
	Fe	16d	5/8	5/8	5/8	1.14(1)
	O	32e	*u*	*u*	*u*	4.00

[a] Cell parameters: $a = 8.362(2)$ Å; $u = 0.381(1)$. Agreement factors: $R_P = 9.05\%$; $R_{wp} = 12.4\%$; $R_{exp} = 6.16\%$; $R_B = 9.13\%$; $\chi^2 = 4.05$; B_{over} (Å^2) = 1.0(2).

(1.46 Å) is much larger than that of Na^+ (1.02 Å).[23] Nevertheless, sodium/ammonium exchanges have been reported to occur in quite different materials such as β-aluminas[24] and sodium molybdates, tungstates, and vanadates.[25,26] Moreover, ammonium "exchange" reactions are now being performed aiming to obtain new materials[27,28] by the subsequent thermal treatment of the exchanged products. The main difference, in our case, seems to be the lack of stability of the ammonium containing products as reflected in step 2.

The final materials obtained through the "exchange" reactions performed either on benzoic acid or ammonium nitrate show the spinel structure and are ferrimagnetic oxyhydroxides. A typical XRD pattern is shown in Figure 1C, and although the crystallinity of these samples is not very good, probably because of the low temperatures at which the exchanges have been performed, the products are clearly spinels. Cell parameters, magnetic moments, and iron distributions are indicated in Table 5. Crystallographic data corresponding to the sample exchanged in benzoic acid are collected in Table 6. The experimental occupation factors of positions 8a and 16d are much lower than the ideal values, 1 and 2, respectively, and therefore, these materials are hypostoichiometric. The exchanged product, $HFeO_2$, can better be formulated as an oxyhydroxide, FeOOH, and this can be reformulated as spinel as $\square Fe_{x(tet)}Fe_{2-x(oct)}O_2(OH)_2$, where the presence of one iron vacancy per formula unit compensates the charge defect created by the OH^-/O^{2-} replacement in the anionic spinel sublattice. For the particular sample analyzed in Table 6, the spinel formulation would give $\square Fe_{0.86(tet)}Fe_{1.14(oct)}O_2(OH)_2$. This hypostoichiometry also affects the magnetic properties.

The product obtained through ammonium nitrate has been formulated as "$\square_{3-z}Fe_zO_{3z-4}(OH)_{8-3z}$" to stress the presence of iron vacancies and the oxyhydroxide character of this phase. Nevertheless, the low crystallinity of the sample does not allow us to use the Rietveld method.

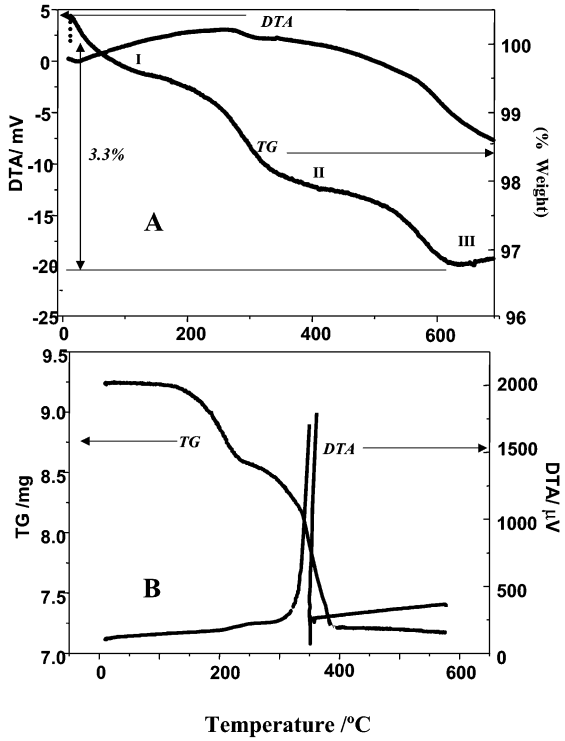

Figure 5. Thermal analysis (in air) of hypostoichiometric samples exchanged in ammonium nitrate (A) and exchanged in benzoic acid (B).

Figure 2B shows a Mössbauer spectrum of a representative sample, where the characteristic sextet of the magnetic ordering can be seen. The spectra adjustment shows the existence of two iron species with two different crystallographic environments, tetrahedral and octahedral. The values of the hyperfine parameters correspond to iron(III) in these two positions, similar to the values corresponding to γ-Fe_2O_3, with spinel structure. These products are ferrimagnetic as shown in the magnetization versus temperature curve of the same sample (Figure 3B), and the experimental effective magnetic moments per formula unit are again in good agreement with the calculated ones, assuming the Néel collinear model and using the iron distribution as deduced from Mössbauer analysis.

As a final comment, these oxyhydroxide ferrites lose some weight if heated, as seen by TGA. They all dehydroxylate at about 300 °C, which is typical for iron oxyhydroxides.[29] Figure 5A shows the TGA and DTA curves corresponding to an ammonium exchanged sample: three different regions

(23) Shannon, R. D.; Prewitt, C. T. *Acta Crystallogr.* **1969**, *B25*, 925.
(24) Kummer, J. T. *Inorg. Synth.* **1995**, *30*, 239.
(25) Grenier, J. C.; Bassat, J. M.; Doumerc, J. P.; Etourneau, J.; Fang, Z.; Fournes, L.; Petit, S.; Pouchard, M.; Wattiaux, A. *J. Mater. Chem.* **1999**, *9*, 25.
(26) Petit, S.; Doumerc, J. P.; Grenier, J. C.; Séguelong, T.; Pouchard, M. *C. R. Acad. Sci.* **2000**.
(27) Gérand, B.; Novogrocki, G.; Guenot, J.; Figlarz, M. *J. Solid State Inorg. Chem.* **1979**, *29*, 429.
(28) Doumerc, J. P.; Grenier, J. C.; Pouchard, M.; Petit, S. French Patent, 95-001875, 1995.
(29) Schwertmann, U.; Cornell, R. M. *Iron Oxides in the Laboratory*; VCH: Weinheim, 1991.

can be distinguished: I (25−150 °C), corresponding to the loss of superficially adsorbed species (<1%, mostly water); II (150−350 °C), corresponding to the dehydroxylation process, which results in the formation of an oxide similar to γ-Fe_2O_3, maghemite; and III (350−600 °C), which results in hematite, α-Fe_2O_3, as the final product. For this particular sample, the observed weight loss of about 3% would correspond to a low content of hydroxyl groups and a *z* value in the previously mentioned formula, step 2, close to 2.5. Although the latter phase transition might be expected to involve no weight loss, it is well documented in the literature that some water can be lost upon heating maghemite, probably because of the presence of residual hydroxide anions; that is, maghemite may retain some oxyhydroxide character.[29,30] It is interesting to note that the oxide similar to maghemite obtained by these means is quite different in character from commercial material. For γ-Fe_2O_3, the magnetic parameters found in the literature are the following: coercivity (H_c) = 250−400 Oe, saturation magnetization M_s = 70 emu/g, and remanent magnetization M_R = 34 emu/g. In our case, for a material obtained by the "exchange" reaction with molten benzoic acid and further thermal treatment at 300 °C, these values are 50 Oe, 28.8 emu/g, and 3.9 emu/g, respectively.

Figure 5B shows the TGA and DTA curves (in air) corresponding to a benzoic acid exchanged material. The weight loss happens in two steps (≈20%), below 200 °C and 400 °C, respectively, the second one being accompanied by a very strong exothermic effect in the DTA plot which does not appear when the experiments are performed in flowing nitrogen. This is, as confirmed by IR experiments, due to the combustion of organic matter carried down and is difficult to eliminate.

To confirm that these ferrites are oxyhydroxides and because O^{2-} and OH^- ions cannot readily be distinguished using XRD, we have performed transmission infrared experiments. The IR spectra corresponding to the ammonium exchanged samples are similar to those corresponding to the previously reported[13] benzoic acid exchanged samples.

The morphology of the oxide obtained by these means appears in Figure 6: the particles are laminar, showing a hexagonal shape reminiscent of the morphology characteristic of the original α-$NaFeO_2$ and quite different from the usual acicular morphology of commercial γ-Fe_2O_3.

(30) Watanabe, H.; Seto, J. *Bull. Chem. Soc. Jpn.* **1993**, *66*, 395.

Figure 6. Scanning electron micrograph of γ-Fe_2O_3 obtained after thermal treatment at 300 °C of an ammonium exchanged ferrite.

4. Summary

We have studied the ferrites obtained by means of different "exchange" reactions performed on α-$NaFeO_2$ in different liquid media: molten salts and molten benzoic acid. Although the working temperatures are variable for the different cases studied, they are much lower than those used in ceramic procedures. Sodium can be replaced by divalent cations (in a 2:1 ratio) or by protons or ammonium ions (1:1 ratio), and in all cases, ferrimagnetic materials showing the spinel structure are obtained. The main difference resides in the stoichiometry as compared to the ideal MFe_2O_4 composition: those ferrites obtained by "exchange" with divalent cations are hyperstoichiometric (that is, they contain occupied interstitial sites), while ferrites obtained by "exchange" with ammonium or protons are hypostoichiometric (that is, they contain an appreciable amount of cationic vacancies). These latter ferrites contain OH^- anions and can be considered as oxyhydroxides; they dehydroxylate at 300 °C yielding a material similar to maghemite, γ-Fe_2O_3. These materials display a lamellar-like morphology.

Acknowledgment. The authors express their gratitude to the Spanish Ministry of Science and Technology (Projects MAT 98-1053 C04-01 and MAT2001-3713-C04-04) for financial support. They are also indebted to Fernando Rojas (UCM) for magnetic measurements and to Dr. M. T. Larrea (UCM) for the ICP analysis.

IC011302K